SLAC-PUB-12892
December 2007
(A)

Simulation Studies on the Vertical Emittance Growth at the Existing ATF Extraction Beamline*

F. Zhou+, J. Amann, S. Selestiky, A. Seryi, C. Spencer, and M. Woodley
SLAC, 2575 Sand Hill Road, Menlo Park, CA 94025, USA

Abstract

Significant dependence of the vertical emittance growth on the beam intensity was experimentally observed at the ATF/KEK extraction beamline. This technical note describes the simulations of possible vertical emittance growth sources, particularly in the extraction channel, where the magnets are shared by both the ATF extraction beamline and its damping ring. The vertical emittance growth is observed in the simulations by changing the beam orbit in the extraction channel even with all optics corrections. The possible reasons for the experimentally observed dependence of the vertical emittance growth on the beam intensity are discussed. An experiment to measure the emittance vs beam orbit at the existing ATF extraction beamline is proposed.

* Work supported by DOE contract DE-AC02-76SF00515
+ E-mail: zhoufeng@slac.stanford.edu

Simulation Studies on the Vertical Emittance Growth in the Existing ATF Extraction Beamline

F. Zhou, J. Amann, S. Selestiky, A. Seryi, C. Spencer, and M. Woodley
SLAC, 2575 Sand Hill Road, Menlo Park, CA 94025, USA

Abstract

Significant dependence of the vertical emittance growth on the beam intensity was experimentally observed at the ATF/KEK extraction beamline. This technical note describes the simulations of possible vertical emittance growth sources, particularly in the extraction channel, where the magnets are shared by both the ATF extraction beamline and its damping ring. The vertical emittance growth is observed in the simulations by changing the beam orbit in the extraction channel even with all optics corrections. The possible reasons for the experimentally observed dependence of the vertical emittance growth on the beam intensity are discussed. An experiment to measure the emittance vs beam orbit at the existing ATF extraction beamline is proposed.

1. Multipole field analysis for the magnets in the ATF extraction channel

A small vertical emittance was experimentally achieved in the ATF/KEK damping ring [1]. However, significant dependence of the vertical emittance growth on the beam intensity was observed [2-3] at the ATF extraction beamline when the beam was extracted from the damping ring. Magnets in the extraction channel, such as QM7R and BS1X, shared by both the extraction beamline and the damping ring, as shown in Fig. 1, are probably one of major nonlinear magnetic field sources that create the emittance growth. The extracted beam has a nominal horizontal deviation from the magnet centers, 0.022 m for QM7R and 0.0855 m for BS1X, and the magnetic fields of both magnets are modeled with the 2-D Poisson program, as shown in Figs. 2 and 3, respectively [4]. The multipoles are decomposed with respect to the nominal position of the extracted-beam using the following equation:

$$B_y + jB_x = B_0 \sum_{n=0}^{\infty} b_n (x + jy)^n \qquad (1)$$

where B_y and B_x are the magnetic field components in y- and x-plane, respectively, j is the imaginary number, B_0 is the normalization constant and b_n is called the 2(n+1)th multipole coefficient. A MathCAD-based built-in function is used to fit the 2-D calculated field, B_x and B_y, as shown in Figs. 4 and 5 for the QM7R and BS1X, respectively. It is shown that the calculated field agrees well with the fitting value, as explained in detail in the plot captions. The corresponding multipole parameters

$K_n L = \frac{L}{B\rho}\frac{\partial^n B_y}{\partial x^n}$ (L is the magnet length and $B\rho$ is the magnetic rigidity) for the QM7R and BS1X are calculated, as given in Table I. It is shown that the sextupoles and octupoles in the QM7R are much stronger than in the BS1X.

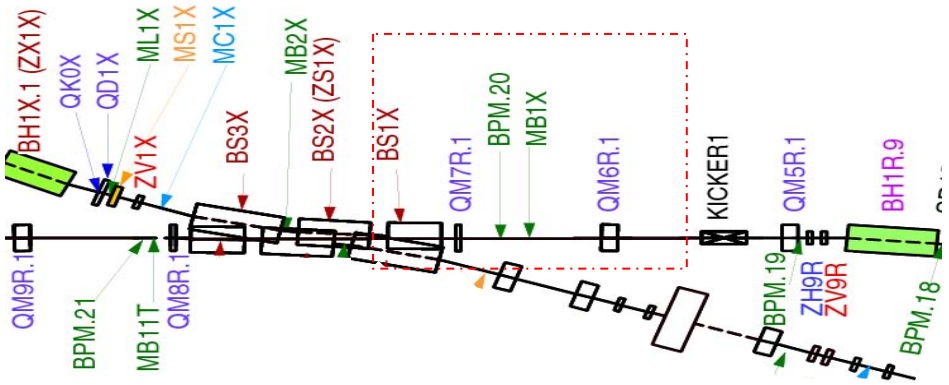

FIG. 1. Schematic of the extraction channel; the magnets within the dashed rectangle in red are shared by both the ATF extraction beamline and the damping ring.

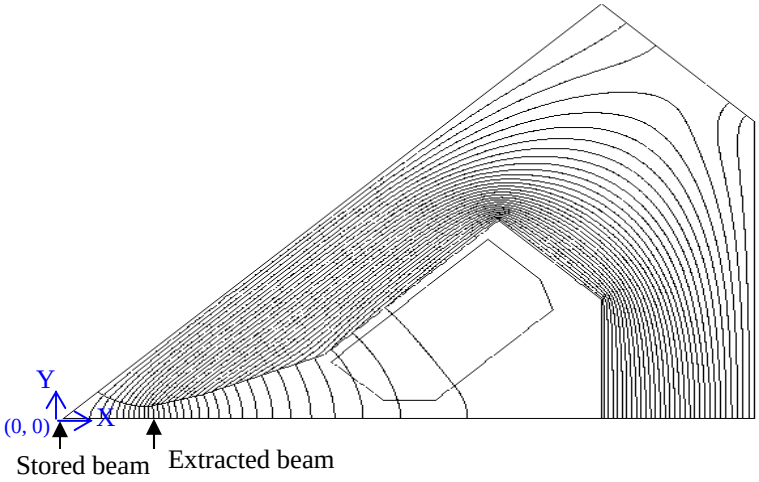

FIG. 2. 1/8 of the QM7R modeled with the Poisson program; the extracted beam is located at X=0.022 m from the magnet center and at Y=0, and the stored beam is at the magnet center, X=0 and Y=0.

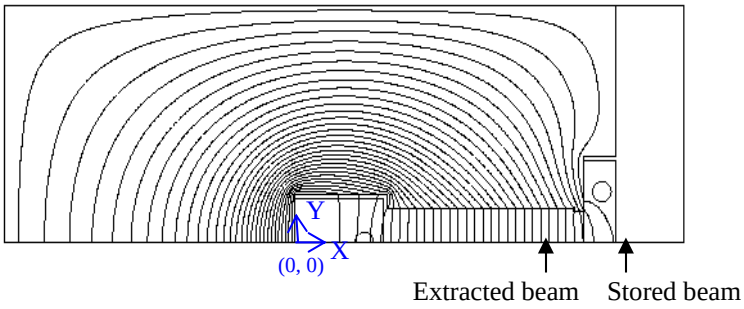

FIG. 3. Top half of the BS1X modeled with the Poisson program; location of the extracted beam is at X=0.0855 m and Y=0.

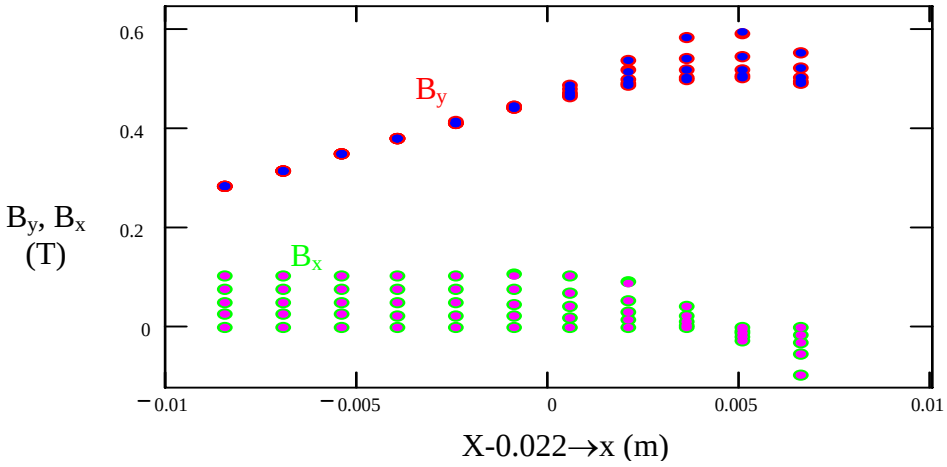

FIG. 4. QM7R magnetic field mapping for B_y and B_x in the new coordinate system x=X-0.022 and y=Y. At each x position, both B_x and B_y have five field data with different y-offset from 0 to 0.005 m; the points in blue and red represent calculated data and fitting value for B_y, and the ones in green and pink represent calculated data and fitting value for B_x. Note that the nominal position of the extracted beam is at x=0 and y=0 in the new coordinate system.

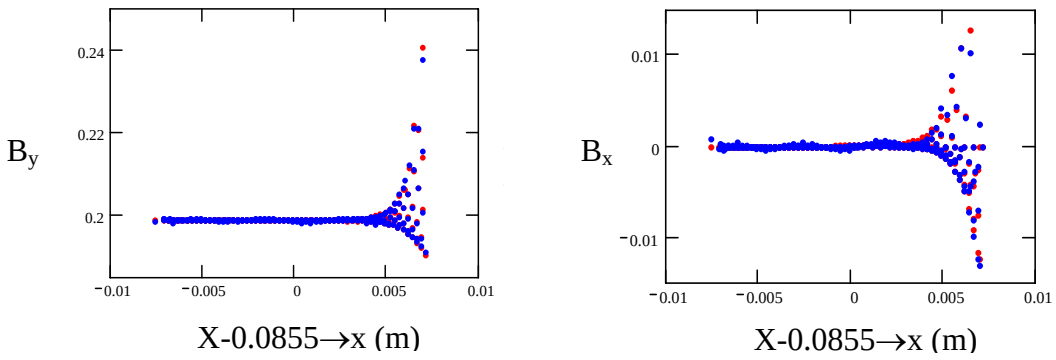

FIG. 5. BS1X magnetic field mapping for B_y (left) and B_x (right) in the new coordinate system x=X-0.0855 and y=Y. At each x position, both B_x and B_y have a few field data with different y-offset from 0 to 0.00375 m; calculated data (blue) agrees with fitting value (red). Note that the nominal position of the extracted beam is at x=0 and y=0 in the new coordinate system.

Table I. Multipole parameters of the QM7R and BS1X.

Multipoles	QM7R	BS1X
K_0L	0.008	0.028
K_1L	0.3201	1.155×10^{-3}
K_2L	-26.601	0.34
K_3L	-1.185×10^{4}	59.216
K_4L	-3.230×10^{6}	-1.889×10^{5}
K_5L	8.205×10^{8}	-1.072×10^{9}
K_6L	1.468×10^{12}	-1.445×10^{12}
K_7L	4.527×10^{14}	-2.242×10^{15}
K_8L	-4.316×10^{17}	-4.563×10^{18}
K_9L	-4.456×10^{20}	-3.394×10^{21}

2. Tracking with the multipoles of QM7R and BS1X

2.1 Local bump generation

The nominal position of the extracted beam traversing through the QM7R and BS1X is at x=y=0 in the new coordinate system described in Figs. 4 and 5. But, in the practical beam operations the beam may deviate from the nominal position and experience strong nonlinear field. For the purpose of modeling the beam at different orbit in the channel, local bumps in x- and y-plane are generated, as shown in Fig. 6, by using six correctors including three horizontal and three vertical correctors. Two vertical correctors, ZV9R and ZV1X, and another two horizontal correctors, ZH9R and ZX1X, already exist in the extraction beamline. Other two correctors, horizontal corrector ‘Hadd’ and vertical

corrector ‘Vadd’, need to be installed immediate upstream of the QM7R. The maximum corrector strength of 10^{-3} T.m is required for the generation of about 1-mm transverse offset at the QM7R.

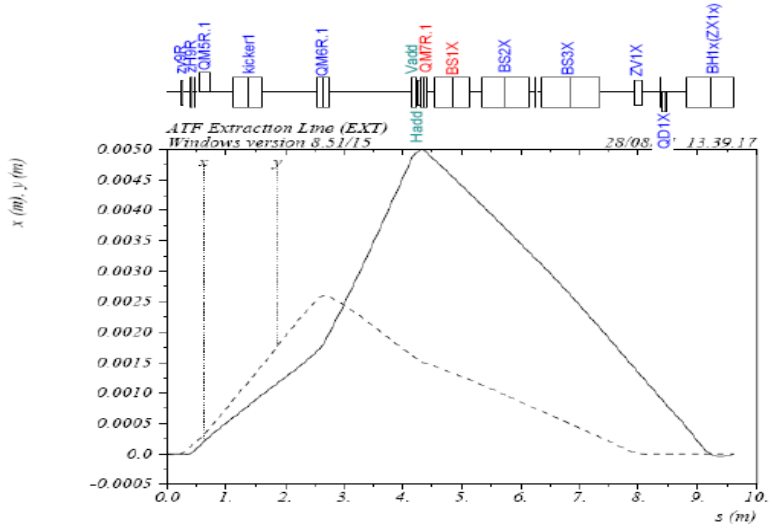

FIG. 6. Generation of local bumps in the x- and y-plane in the extraction channel. The bump amplitudes at the QM7R are adjustable by tuning the correctors.

2.2 Tracking with the multipole fields

The multi-particle tracking is extensively performed using the MAD, along the existing beamline starting from the ZV9R in the damping ring to the end of the coupling correction and wire scanners station in the extraction beamline. The following nominal initial parameters are used for the tracking: 5 μm of normalized horizontal emittance, 30 nm of normalized vertical emittance, 8 mm of bunch length, and 0.08% of the energy spread. The starting Twiss parameter at the ZV9R is exactly taken from the damping ring lattice. At this stage, all magnet errors are not included in this tracking except the multipoles of the QM7R and BS1X. The transverse offset discussed in the next sections is measured at the QM7R in the new coordinate system and the emittance is measured at the end of the extraction beamline.

2.2.1 Vertical emittance with x- or y-offset

Without optics correction, the normalized vertical emittance vs x- or y-offset from the nominal position without and with multipoles is compared, as shown in Fig. 7. It shows that the vertical emittance keeps constant as x-offset increases (Fig. 7a). But, the emittance is significantly increased as y-offset increases (Fig. 7b), and also the emittance growth is dominantly caused by the multipoles.

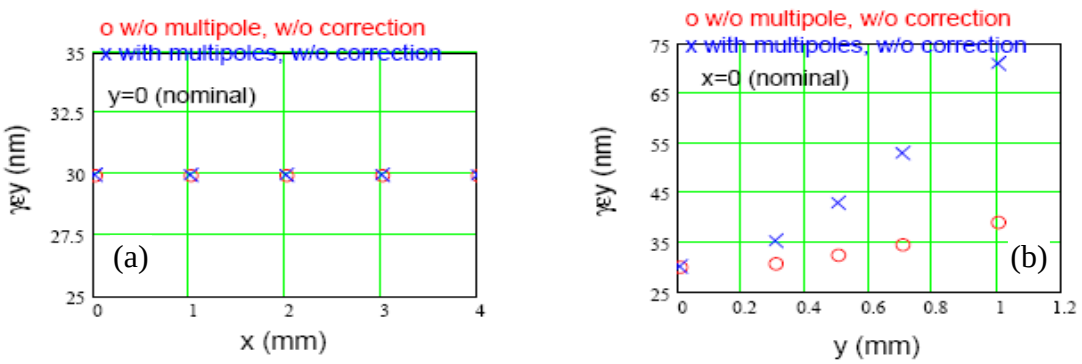

FIG. 7. Normalized vertical emittance vs x-offset (a) or y-offset (b) without any optics correction; the results of without and with multipoles are compared.

2.2.2 Vertical emittance with x- and y-offset

Fig. 8 shows the vertical emittance of both x- and y-offset without and with optics corrections for dispersion, coupling and Twiss. The tracking results are also compared for the cases of without and with multipoles. For the case of without multipoles, shown in Fig. 8a, the emittance growth keeps constant at y=1 mm offset since the coupling is not changed, while in Fig. 8b it shows that the emittance is increased as y-offset becomes large. For the case of with multipoles, the vertical emittance is increased by 50% with the offset of x=5 mm and y=1.5 mm even with all optics corrections.

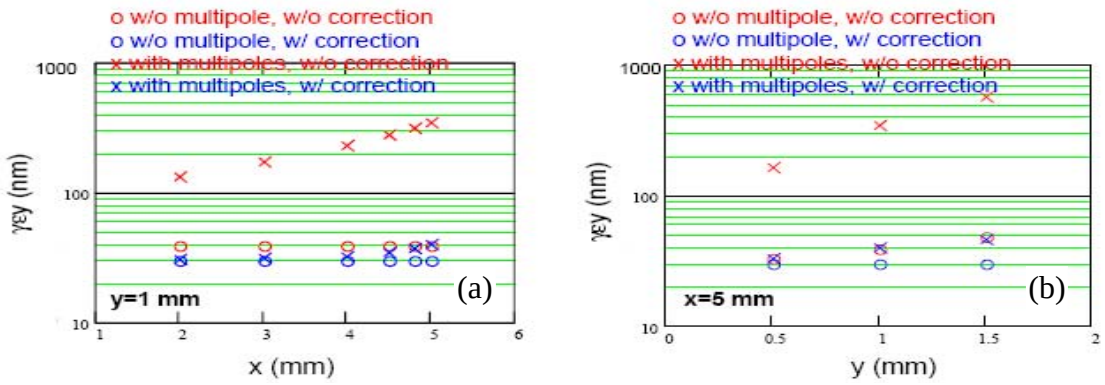

FIG. 8. The normalized vertical emittance vs x- and y-offset without and with optics corrections; the results of without and with multipoles are compared.

2.2.3 Transverse phase spaces with beam offset

The phase spaces of a beam at the nominal position (green), at y=1 mm offset (red) and at x=5 mm offset (brown), are shown in Fig. 9(a). It shows that the phase space of x=5 mm offset is very close to the one at the nominal position, which agrees well with the analytical estimate using Hamiltonian [5], while the one with y=1 mm offset blows up,

where the beam experiences strong coupling effects. Fig. 9(b) shows the vertical phase spaces of a beam at the nominal position (green), combined offset of x=5 mm and y=1 mm (red), and x=-5 mm and y=1 mm (brown). It is shown that the phase space volume significantly increases in the offset of x=5 mm and y=1 mm while the one with offset of x=-5 mm and y=1 mm is close to the one at the nominal position. The reason is that the magnetic field in the offset of x=5 mm and y=1 mm is in strong nonlinear region while the one in the offset with x=-5 mm and y=1 mm is in linear region, which may not dilute the phase space. Figs. 9(c) and 9(d) show the phase space y-y′ and x-y of a beam at the nominal position, combined offset of x=5 mm and y=1 mm without correction (red) and with corrections (brown), respectively. The coupling is corrected well based on the phase space of x-y (d) in brown, but its corresponding phase space of y-y′ (c) in brown blows up.

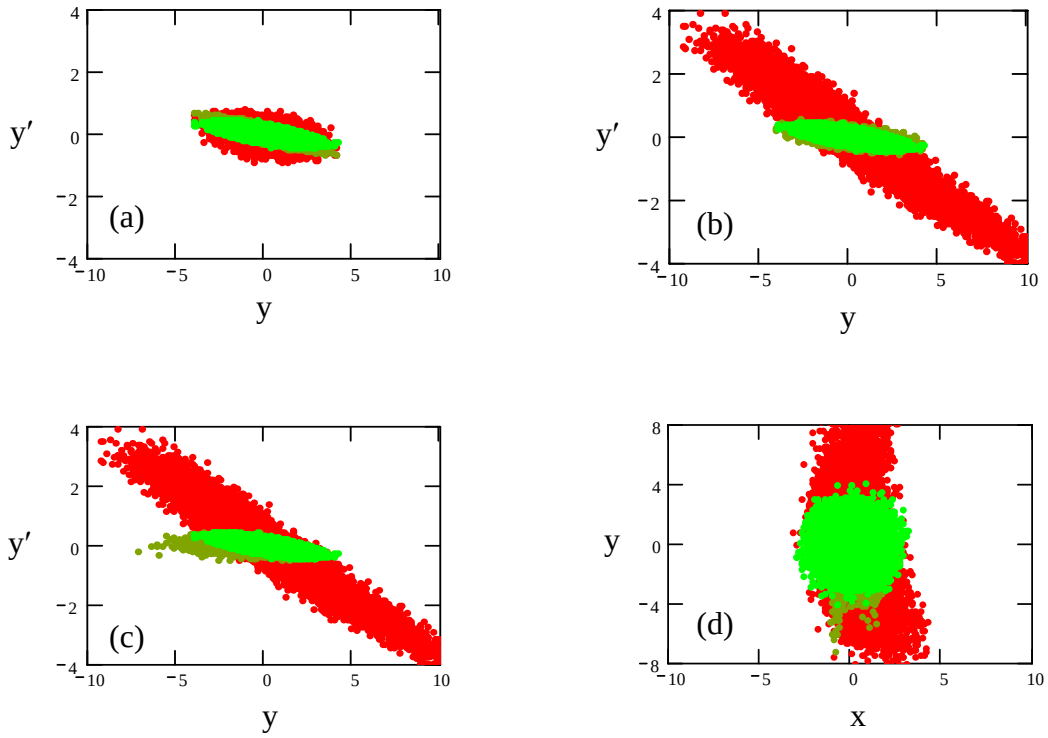

FIG. 9. The phase spaces with different transverse offset. The plot (a) corresponds to a beam at the nominal position (green), at y=1 mm offset (red), and at x=5 mm offset (brown); the plot (b) represents a beam at the nominal position (green), at combined x=-5 mm and y=1 mm offset (brown), and combined x=5 mm and y=1 mm offset (red); the plots (c) and (d) show the phase space y-y′ and x-y of a beam at the nominal position, at combined offset of x=5 mm and y=1 mm without correction (red), and with corrections (brown), respectively.

2.2.4 Dependence of the emittance growth on the beam intensity

Both the transverse wakefield and energy spread depend on the beam intensity. One possible reason for the experimentally observed dependence of the vertical emittance growth on the beam intensity is that the transverse beam offset is probably created by the transverse wakefield. The simulation also shows that the vertical emittance blows up as the energy spread increases; so the emittance dependence on the energy spread is another possible reason for its dependence on the beam intensity.

2.3 Proposal of a beam experiment at the existing ATF extraction beamline

In order to understand vertical emittance growth source and how well the coupling is corrected using the existing coupling correction setup, we propose to measure transverse phase space of an extracted beam traversing through local bumps in the channel. Most hardware to generate local bumps already exists except two correctors near QM7R, 'Hadd' and 'Vadd', which need to be installed. Emittance can be measured at the emittance station using existing laser wire scanners. The orbit generated by the ZV9R, ZH9R, 'Hadd' and 'Vadd', can be closed up in the ATF damping ring for the stored beam by using the correctors ZH10R, ZV10R, ZH11R, and ZV11R downstream of the QM7R, as shown in 10. To close up the orbit for the injected beam in the beam transport beamline looks feasible and further investigation is underway [6].

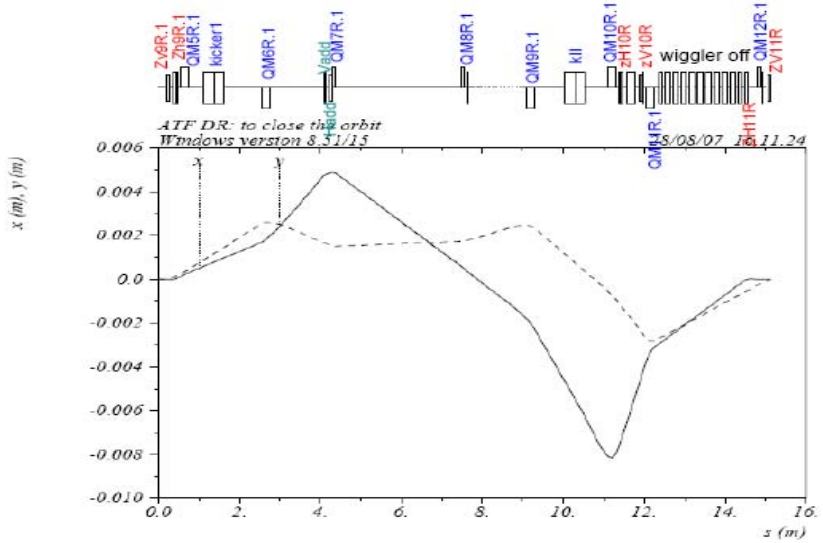

FIG. 10. Closed orbit for the stored beam in the damping ring using existing correctors.

3. Summary

The possible source to dilute the vertical emittance at the existing ATF extraction beamline is investigated. The vertical emittance growth is observed in the simulations by changing the beam orbit in the extraction channel, where the magnets are shared by both the ATF damping ring and the extraction beamline, even with all optics corrections. The reasons for the experimentally observed dependence of the vertical emittance growth on the beam intensity are discussed. An experiment to measure the emittance vs beam orbit at the existing ATF extraction beamline is proposed.

Acknowledgements

We would like to thank many KEK and LAL colleagues for the helpful discussions and suggestion.

References

[1] K. Kubo, *et al*., PRL 88, 194801 (2002).
[2] J. Nelson, M. Ross, M. Woodley, ATF-00-06, June 2001.
[3] S. Kuroda, ATF2 project meeting, March 2007.
[4] C. Spencer, ATF2 meeting at SLAC, March 2007.
[5] S. Kuroda, ATF2 weekly-meeting, June 2007.
[6] M. Woodley, private communication, September 2007.